

Thermal radiation method: proposal of a new technique for measuring interfacial or surface fluctuations

Y. Kajihara,^{a*} Y. Ohmasa^b and M. Yao^b

^aGraduate School of Integrated Arts and Sciences, Hiroshima University, Higashi-Hiroshima 739-8521, Japan, and ^bDepartment of Physics, Graduate School of Sciences, Kyoto University, Kyoto 606-8502, Japan.
Correspondence e-mail: kajihara@hiroshima-u.ac.jp

Received 16 August 2006
Accepted 28 November 2006

A thermal radiation method is proposed as a new technique for measuring interfacial or surface fluctuations. From Kirchhoff's law, the intensity includes diffuse scattering, which means that it can be used to measure mesoscopic fluctuations of samples like a small-angle X-ray or neutron scattering method. We applied the method to mercury on a sapphire system where the mercury wets the sapphire by a first-order phase transition (prewetting) at high temperature and high pressure, and thus large fluctuations in the film can be expected in its supercritical region. We succeeded in measuring huge surface fluctuations in the film.

© 2007 International Union of Crystallography
Printed in Singapore – all rights reserved

1. Introduction

What information is contained in the thermal radiation from a body? How it can be utilized in an experiment? Its intensity is well known to follow Planck's law and has been used to measure the temperature of the sample. Its intensity is also known to contain optical reflectivity and absorption coefficient terms, which have been utilized to detect film thickness during film deposition by molecular beam epitaxy (SpringThorpe *et al.*, 1989), to measure the surface polariton mode in Si-based surface structure of the order of micrometres (Hesketh *et al.*, 1986; Greffet *et al.*, 2002), and to confirm optical absorption features of artificially made photonic crystals (Cornelius & Dowling, 1999; Lin *et al.*, 2000). The radiation intensity, moreover, contains a diffuse scattering term (Landau & Lifshitz, 1958), which means that it can be utilized to study mesoscopic fluctuations like a small-angle X-ray or neutron scattering method. We applied this new technique to a special system: surface fluctuations in a liquid mercury film on a sapphire system in which the prewetting transition occurs at high temperature and high pressure.

2. Thermal radiation

It is well known that the intensity of thermal radiation from a black body is formulated by Planck's law. When the object is *not* a black

body, the formula is corrected by Kirchhoff's law. From this law, the intensity of the radiation from the body I_{rad} emitted at a finite solid angle $\Omega(\theta, \phi)$ (θ and ϕ are the polar and azimuthal angles, respectively) is proportional to the absorbing power of the body A (Landau & Lifshitz, 1958):

$$I_{\text{rad}} = I_{\text{BB}} A(\lambda, \theta) \cos \theta. \quad (1)$$

Here I_{BB} denotes the intensity of the black-body radiation. The absorbing power is the ratio of the light absorbed to the light which is incident on the body and depends on the wavelength λ and polar angle θ .

This formulation is easily understood by the following consideration: a body is surrounded by the black body and is in thermal equilibrium to it as shown in Fig. 1. From the black body, (Planck's) black-body radiation $I_{\text{BB}} \cos \theta$ is emitted towards a unit surface area of the body. It is partially reflected [reflectivity $R(\theta)$] and is scattered (scattering cross section $d\sigma/d\Omega'$) at the surface of the body. From the body, the radiation I_{rad} is emitted towards the black body. These radiations should be balanced in each solid angle $\Omega(\theta, \phi)$ because the system is in thermal equilibrium and thus

$$I_{\text{BB}} \cos \theta = I_{\text{BB}} \cos \theta R + I_{\text{BB}} \int d\Omega' \frac{1}{S} \frac{d\sigma}{d\Omega'} + I_{\text{rad}} \cos \theta, \quad (2)$$

therefore

$$e(\lambda, \theta) \equiv \frac{I_{\text{rad}}(T, \lambda, \theta)}{I_{\text{BB}}(T, \lambda)} = [1 - R(\lambda)] \cos \theta - \int d\Omega' \frac{1}{S} \frac{d\sigma}{d\Omega'}, \quad (3)$$

where S denotes the surface area of the body and e is called the emissivity. In this case, the absorbing power corresponds to

$$A = 1 - R - \int d\Omega' \frac{1}{S \cos \theta} \frac{d\sigma}{d\Omega'}. \quad (4)$$

This formulation means that the radiation measurement is equivalent to a light scattering measurement by integrating all the scattered angles. The momentum transfer of the light scattered to a finite (properly large) angle corresponds to that of X-ray or neutron small-angle or grazing-incident scattering methods. Therefore we propose

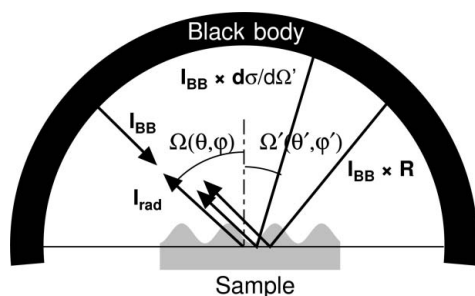


Figure 1
A simple model to explain Kirchhoff's law. When the sample is in thermal equilibrium with the surrounding black body, the radiations from both bodies and the reflected and diffuse-scattered light at the surface of the sample should be balanced. See text for details.

that the radiation method can be substituted for these scattering methods (Fig. 2).

3. Prewetting transition

The prewetting transition is a first-order phase transition between thin and thick film with mesoscopic order and has its own critical point [for a review see Bonn & Ross (2001)]. It was first observed in a He on Cs system and now several other systems are known. The order parameter is film thickness (strictly speaking, coverage) and thickness fluctuations, which indeed have not been reported, are naturally expected in the supercritical region like density fluctuations for a liquid–gas transition. Hg on sapphire is one of such prewetting systems and we have studied the average properties of the film by optical reflectivity measurements before (Ohmasa *et al.*, 2001). However, it is very difficult to study the fluctuations in the film by X-ray, neutron or light scattering methods, because the prewetting critical point of the system is located at extreme conditions of temperature $T_{CPW} = 1741$ K and pressure 159 MPa. Thus other methods are inevitable and we applied the new radiation method to this system.

4. Experiment

The experimental setup is shown in Fig. 3(a). A mercury sample was encapsulated in a cylindrical molybdenum cell. A sapphire rod, which served as an optical window as well as the substrate of the mercury

wetting film, was inserted from one end of the cell. The central part of the cell could be heated by two molybdenum heaters up to 1803 K and the temperature was measured by W–Re thermocouples. The cell was put in a high pressure vessel and pressurized with argon gas. We could achieve a high pressure state up to 200 MPa. We measured the thermal radiation emitted from the sample to its normal [$\theta = 0$ in equation (2)] using the two spectrometers; they were equipped with an Si charge coupled device (CCD) and an (In,Ga)As photodiode (PD) array whose sensibility wavelength ranges were $300 < \lambda < 1000$ and $900 < \lambda < 1550$ nm, respectively. We also measured the reflectivity by using a He–Ne laser (wavelength 633 nm) as a light source and a photomultiplier (PM) as a detector. Further details of the experimental setup are shown in other papers (Ohmasa *et al.*, 2001; Kajihara *et al.*, 2003).

The measurements were carried out over wide temperature and pressure ranges up to 1803 K and 200 MPa including the prewetting supercritical region by decreasing (or increasing) the pressure at constant temperatures. From the measured radiation intensity I_{obs} , we obtained the emissivity as

$$e = I_{obs}/I_{BB}(T), \tag{5}$$

where T was the sample temperature measured by thermocouples when the sample was opaque. When it became *not* opaque, the observed radiation intensity I_{obs} consisted of not only that from the sample I_{sample} but also that from the cell behind the sample I_{cell} as shown in Fig. 3(b). Note that in this context, the *sample* indicates not only an Hg wetting film (a few to 10 nm thickness) but also bulk Hg (about 5 mm thickness) behind the film. The observed radiation intensity was expressed as (Kajihara *et al.*, 2003)

$$I_{obs} = I_{sample}[1 - \exp(-\alpha L)] + I_{cell} \exp(-\alpha L), \tag{6}$$

where α and L denote the absorption coefficient and the length of the sample, respectively. Thus we corrected the emissivity as

$$e = \frac{I_{sample}}{I_{BB}} = \frac{I_{obs} - I_{cell} \exp(-\alpha L)}{1 - \exp(-\alpha L)} \frac{1}{I_{BB}}. \tag{7}$$

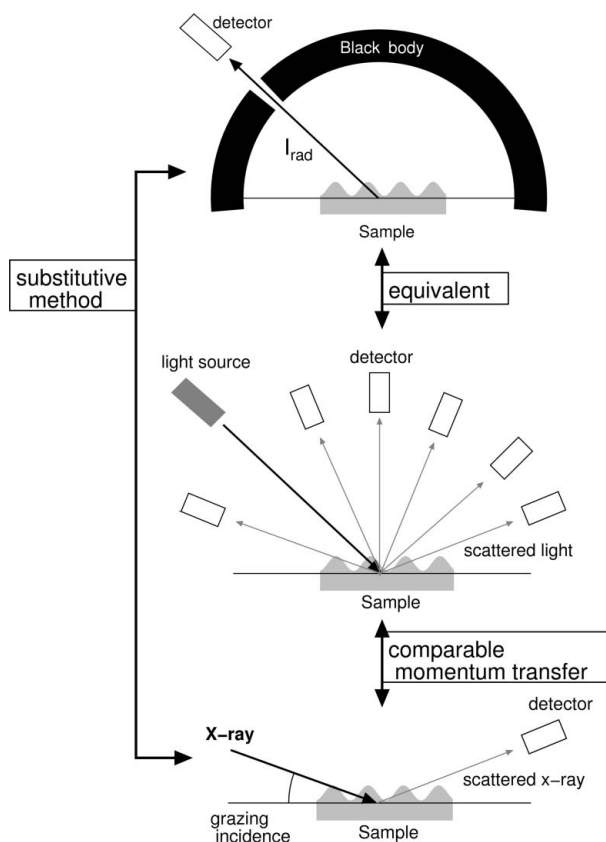


Figure 2 Relationship between the thermal radiation and grazing incident scattering methods: the former can be substituted for the latter because the former is equivalent to the light scattering method, whose momentum transfer is comparable to the latter. See text for details.

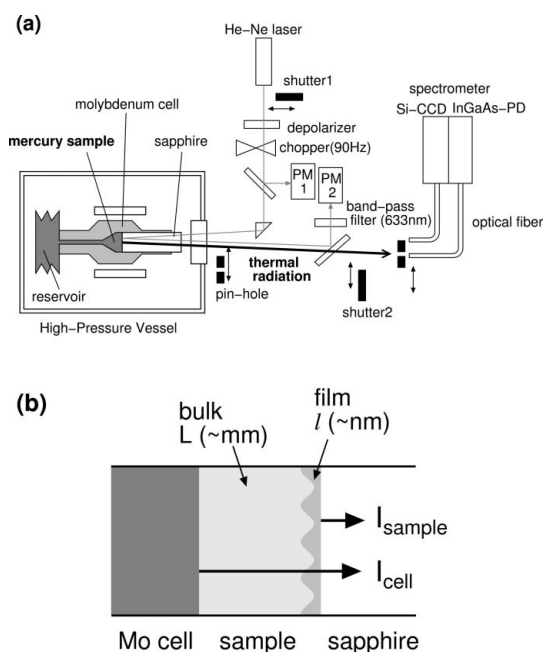


Figure 3 (a) Experimental setup for the simultaneous measurements of the emissivity and reflectivity and (b) schematic illustration around the sample.

In this calculation, we used I_{cell} which was estimated from the measured radiation intensity when the sample was nearly transparent ($\alpha \simeq 0$) by $I_{\text{cell}} = I_{\text{obs}}$.

5. Results

The representative results are shown in Fig. 4: (a), (b) and (c), (d) indicate the reflectivity and emissivity at 1678 and 1775 K where the temperature is in the *subcritical* and *supercritical* regions, respectively.

In Fig. 4(a), the reflectivity shows high values above 136 MPa where the sample is bulk liquid. With decreasing pressure, it shows discontinuous decreases at 136 and 134 MPa, which correspond to the liquid–gas and prewetting transitions, respectively; at the prewetting transition, the thickness of the Hg film formed on the sapphire changed from thick to thin discontinuously. In contrast to the reflectivity, the emissivity in Fig. 4(b) shows smaller values in the liquid state and higher values in the gaseous state with the wetting film. This can be explained qualitatively *via* the relation $e = 1 - R$. In Fig. 4(c), the reflectivity changes continuously because the temperature is higher than the liquid–gas critical temperature $T_C = 1751$ K and the property of Hg changes continuously. The reflectivity shows a minimum around 167 MPa, where the refractive index of bulk Hg is equal to that of sapphire. On the other hand, the emissivity shows a substantial dip with a minimum around 150–160 MPa. This dip cannot be explained by the term $1 - R$, and thus the scattering intensity has to be taken into account. The dip becomes deeper as the wavelength becomes shorter, indicating that the scattering intensity gets larger as the wavelength becomes shorter.

This distinctive behavior of the emissivity can be seen more clearly when it is plotted against the bulk density, which is the most relevant parameter for determining the physical properties (including the optical properties) of the fluid Hg. The reflectivity R_{bulk} at the bulk Hg/sapphire interface, which is calculated from the refractive index of bulk mercury (Kajihara *et al.*, 2003) and that of sapphire (Malitson *et al.*, 1958; Gray, 1972), depends on the Hg density as shown in Fig. 5 by solid lines; (a), (b) and (c) show the values at wavelengths 633, 1000

and 1500 nm. In the same figure, we plotted the density dependence of the emissivity using symbols; different symbols corresponded to the data at different temperatures in the figure; the density was obtained from the measured pressure and temperature according to the Hg phase diagram by Götzlaff (1988). When the density is higher than 7 g cm^{-3} , the emissivity does not depend on temperature and nearly coincides with the solid line, which indicates that the sample is bulk liquid without (or with negligible) wetting film and fluctuations. But below 7 g cm^{-3} , the emissivity *does* depend on temperature and clearly differs from the solid line. Thus we need to consider the scattering term in equation (2).

To deduce the scattering intensity spectrum $\int d\Omega'(1/S \cos \theta)(d\sigma/d\Omega')(\lambda)$ from the results, we further need to know the reflectivity spectrum $R(\lambda)$. We only measured the reflectivity

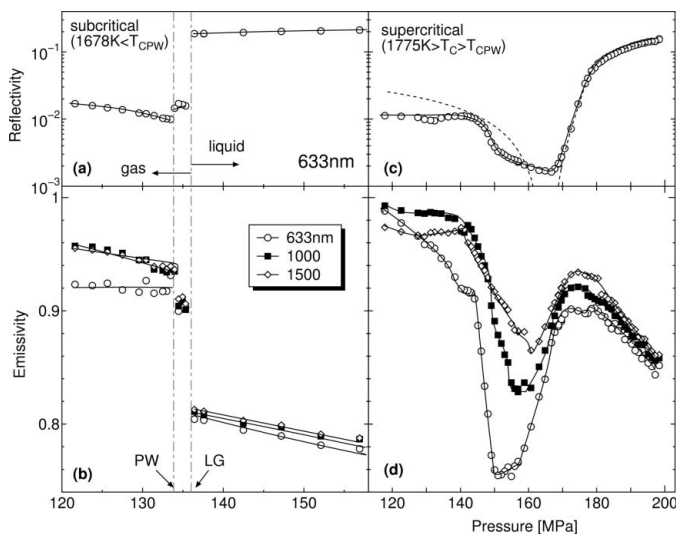


Figure 4 Pressure dependence of the reflectivity and emissivity in the subcritical (a, b) and supercritical (c, d) regions. Dashed lines indicate the calculated reflectivities at the bulk Hg/sapphire interface. LG and PW denote the liquid–gas and prewetting transitions, respectively.

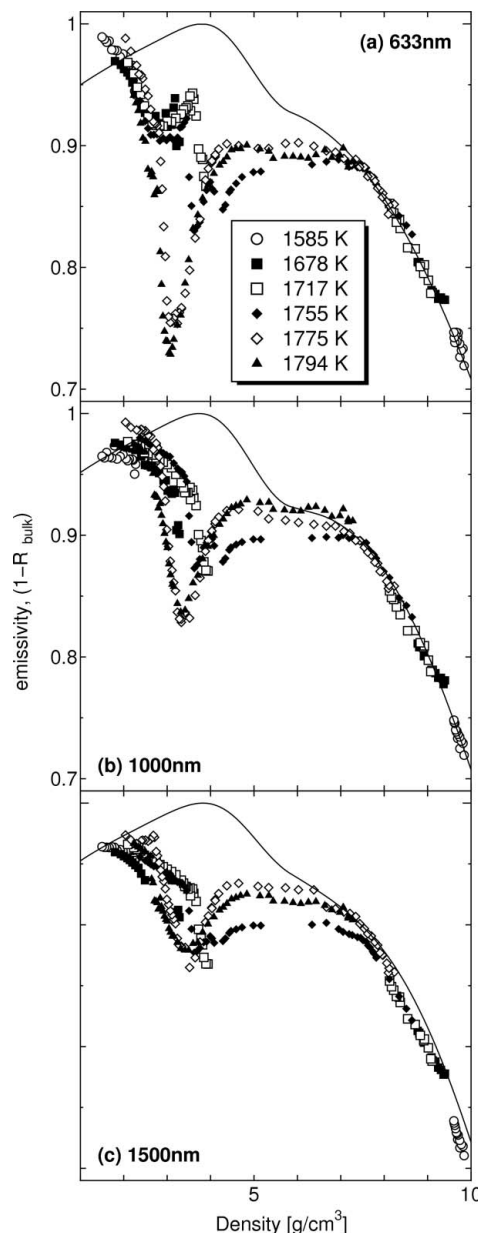


Figure 5 Density dependence of the emissivity at wavelengths (a) 633, (b) 1000 and (c) 1500 nm. Different symbols correspond to the data at different temperatures in the figure. Solid lines indicate the calculated reflectivity at the bulk Hg/sapphire interface.

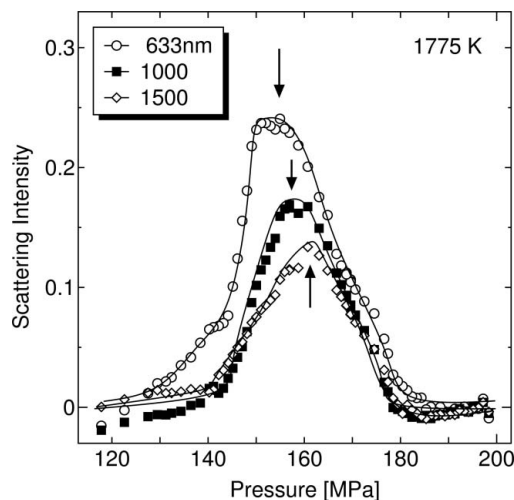


Figure 6
Pressure dependence of estimated scattering intensities at 1775 K. Arrows indicate the points where the scattering intensities show a maximum.

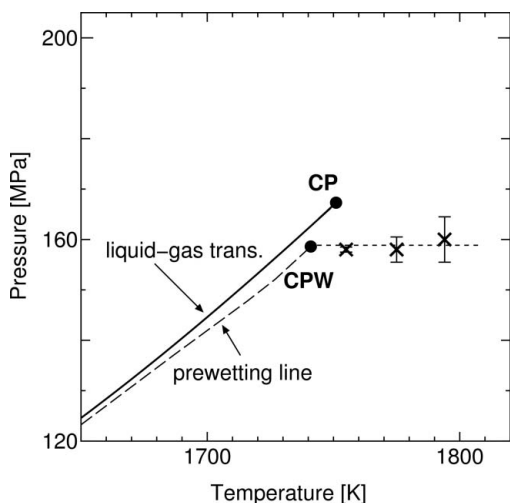


Figure 7
State points where the scattering intensity shows a maximum on the Hg phase diagram. The solid and dashed lines represent liquid-gas and prewetting transitions, respectively. CP and CPW denote these critical points. The dotted line is a guide for the eyes.

tivity $R(\lambda = 633 \text{ nm})$, thus we substituted the calculated bulk value $R_{\text{bulk}}(\lambda)$ for the real $R(\lambda)$. This substitution is guaranteed as shown in Fig. 4; the difference between the real R with a wetting film [open circles in (a) and (c)] and the calculated bulk value R_{bulk} (dashed lines) is very small ($\approx 10^{-2}$) compared with the scattering term (or dip of the emissivity, $\approx 10^{-1}$) at the wavelength 633 nm; the situation should not change much at other wavelengths of interest. Thus the scattering intensity spectrum is obtained as,

$$\int d\Omega' \frac{1}{S \cos \theta} \frac{d\sigma}{d\Omega'} = 1 - e(\lambda) - R_{\text{bulk}}(\lambda). \quad (8)$$

We show representative results at some wavelengths in Fig. 6. The scattering intensity at each wavelength shows a maximum around 150–160 MPa. We plot the state points where the scattering intensity shows a maximum (arrows in Fig. 6) on the Hg phase diagram in Fig. 7 using crosses (because the points are slightly different from each

wavelength, error bars are added). These points are located at the supercritical region of the prewetting transition and fall on a line. Thus the observed scattering should have a strong relationship with the prewetting critical fluctuations.

We tentatively estimated the film fluctuations with some assumptions (Kajihara *et al.*, 2003). Thickness fluctuations Δl reach a few nm and the lateral correlation length ξ_{\parallel} hundreds of nm. These values are huge compared to the thickness l of the Hg film, which is estimated to be about 10 nm by optical reflectivity measurements (Ohmasa *et al.*, 2001). It would be very interesting to elucidate how Δl and ξ_{\parallel} vary with temperature and pressure, or how these fluctuations relate to the prewetting critical fluctuations. However, at the present stage it is very difficult to estimate changes of these values because the accuracy of the data is not high enough and a method for analyzing the emissivity is not established. Theoretical investigations are expected.

6. Conclusions

Thermal radiation measurements of mercury on a sapphire system were carried out at high temperature and high pressure up to 1803 K and 200 MPa. A substantial dip of the emissivity was observed in the prewetting supercritical region. This anomaly can be explained by the fact that the dip is assumed to be derived from the interfacial fluctuations in the mercury wetting film on sapphire.

We propose that this radiation method can be utilized to measure mesoscopic fluctuations and thus can be a substitute for an X-ray or neutron small-angle or grazing incident scattering method. Characteristics of the method are as follows.

Advantage: very simple experimental settings; in particular, no light source is needed.

Disadvantages: (1) A high temperature is needed. In our settings, only data above 1273 K were available. (2) Momentum-transfer-dependent measurement is impossible. Only the wavelength dependence (which is not same as in X-ray or neutron energy dispersion methods because the scattering angle is integrated) can be observed.

Although the disadvantages are difficult to overcome, we expect that the method will be useful for special systems under extreme conditions where ordinary scattering measurements are difficult. Surface fluctuations in levitated liquids and surface melting of materials with high melting temperatures are candidates.

References

- Bonn, D. & Ross, D. (2001). *Rep. Prog. Phys.* **64**, 1085–1163.
- Cornelius, C. & Dowling, J. (1999). *Phys. Rev. A*, **59**, 4736–4746.
- Götzlaff, W. (1988). Doctoral thesis, University of Marburg, Germany.
- Gray, D. E. (1972). *American Institute of Physics Handbook*, 3rd ed. New York: McGraw-Hill.
- Greffet, J.-J., Carminati, R., Joulain, K., Mulet, J.-P., Mainguy, S. & Chen, Y. (2002). *Nature (London)*, **416**, 61–64.
- Hesketh, P., Zemel, J. & Gebhart, B. (1986). *Nature (London)*, **324**, 549–551.
- Kajihara, Y., Ohmasa, Y. & Yao, M. (2003). *J. Phys. Condens. Matter*, **15**, 6179–6198.
- Landau, L. D. & Lifshitz, E. (1958). *Statistical Physics*, §60. New York: Pergamon Press.
- Lin, S.-Y., Fleming, J. G., Chow, E., Bur, J., Choi, K. K. & Goldberg, A. (2000). *Phys. Rev. B*, **62**, R2243–R2246.
- Malitson, I. H., Murphy, F. V. Jr & Rodney W. S. (1958). *J. Opt. Soc. Am.* **48**, 72–73.
- Ohmasa, Y., Kajihara, Y. & Yao, M. (2001). *Phys. Rev. E*, **63**, 051601 (1–14).
- SpringThorpe, A. J., Humphreys, T. P., Majeed, A. & Moore, W. T. (1989). *Appl. Phys. Lett.* **55**, 2138–2140.